

EGFR, and VEGFR inhibitory activities of the crude extract from marine algae *Dictyopteris acrostichoides* supported by in silico analysis and metabolic profiling

Eman Zekry Attia

Minia University Faculty of Pharmacy

Iman A. M. Abdel-Rahman

South Valley University Faculty Of Pharmacy

Omar M. Aly

Port Said University

Hani Saber

South Valley University Faculty of Science

Mohammed Ismael Rushdi (✉ mrushdy258@svu.edu.eg)

South Valley University <https://orcid.org/0000-0001-9488-4019>

Usama Ramadan Abdelmohsen


Minia University Faculty of Pharmacy <https://orcid.org/0000-0002-1014-6922>

Research Article

Keywords: *Dictyopteris acrostichoides*, cytotoxicity, metabolic profiling, in silico, EGFR, and VEGFR

Posted Date: May 10th, 2023

DOI: <https://doi.org/10.21203/rs.3.rs-2854258/v1>

License:  This work is licensed under a Creative Commons Attribution 4.0 International License. [Read Full License](#)

Version of Record: A version of this preprint was published at *Revista Brasileira de Farmacognosia* on October 24th, 2023. See the published version at <https://doi.org/10.1007/s43450-023-00474-8>.

Abstract

Ethanol extracts of *Caulerpa racemosa*, *Dictyopteris acrostichoides*, *Halimeda opuntia* and *Polycladia myrica*, were tested for their cytotoxicity against HepG2 (human hepatoma), MCF-7 (human breast adenocarcinoma), and Caco-2 (human colon adenocarcinoma) cells. *Dictyopteris acrostichoides* displayed cytotoxicity against HepG2, MCF-7 and Caco-2 with IC₅₀ values of 11.65, 9.28 and 16.86 µg/mL, respectively in comparison to doxorubicin as a positive control, (IC₅₀ = 5.72, 5.17 and 5.81 µg/mL, respectively). LC-HR-ESI-MS metabolic profiling of the *D. acrostichoides* extract characterized seventeen metabolites (**1–17**). In silico analysis indicated 1-(3-oxo-undecylidithiyl)-undecan-3-one (**16**) was the most active EGFR inhibitor, while 1-(3-Oxo-undecylidithiyl)-undecan-3-one (**16**) and di(3-acetoxy-5-undecenyl) disulfide (**17**) were the most active VEGFR inhibitors. Furthermore, the ethanol extract of *D. acrostichoides* was tested against epidermal growth factor receptor (EGFR) kinase (IC₅₀ = 0.11 µg/mL) compared to lapatinib as a positive control, (IC₅₀ = 0.03µg/mL) and against vascular endothelial growth factor (VEGF) (IC₅₀ = 0.276 µg/mL) compared to sorafenib as a positive control, (IC₅₀ = 0.049 µg/mL).

Highlights

1. Ethanol extracts of *Caulerpa racemosa*, *Dictyopteris acrostichoides*, *Halimeda opuntia* and *Polycladia myrica* were tested for their cytotoxicity against HepG2 (human hepatoma), MCF-7 (human breast adenocarcinoma), and CACO-2 (human colon adenocarcinoma) cells.
2. *D. acrostichoides* ethanol extract displayed cytotoxicity against HepG2, MCF-7 and CACO-2 (IC₅₀= 11.65, 9.28 and 16.86 µg/mL, respectively) compared to doxorubicin as a positive control, (IC₅₀= 5.72, 5.17 and 5.81 µg/mL, respectively).
3. *D. acrostichoides* ethanol extract was tested against epidermal growth factor receptor (EGFR) kinase (IC₅₀= 0.11 µg/mL) compared to lapatinib as a positive control, (IC₅₀ = 0.03µg/mL) and against vascular endothelial growth factor (VEGF) (IC₅₀= 0.276 µg/mL) compared to sorafenib as a positive control, (IC₅₀= 0.049µg/mL).
4. LC-HR-ESI-MS metabolic profiling of *D. acrostichoides* ethanol extract characterized seventeen metabolites.
5. In silico analysis indicated 1-(3-oxo-undecylidithiyl)-undecan-3-one was the most active EGFR inhibitor, while 1-(3-Oxo-undecylidithiyl)-undecan-3-one and di(3-acetoxy-5-undecenyl) disulfide were the most active VEGFR inhibitors.

1. Introduction

Malignant tumors are an extremely serious public health problem that has aroused worldwide attention, thus discovering antitumor drugs becomes as a research hotspot. Phytochemical researchers investigated the cytotoxic capacity of phytochemicals in opposition to variable most cell lines. Seaweed expressed an exceptionally treasured supply of novel bioactive substances that may power the results of various drugs (Zhu et al. 2019). Among the therapeutic targets for cancer, the abnormal expression of the epidermal growth factor receptor (EGFR) is strongly associated with various malignancies such as breast, ovarian, non-small-cell lung, prostate, and colon cancers. The EGFR has been confirmed to be closely related to tumor growth, progression, and metastasis. The poor prognosis of cancer patients prompts extensive studies on the EGFR signaling pathway (Allam et al. 2020). Increasing evidence has shown that EGFR inhibitors have great potential in the treatment of tumors, especially non-small-cell lung cancer, hepatocellular carcinoma, and pancreatic cancer, which has inspired a research boom based on the design and synthesis of EGFR inhibitors (Hassan et al. 2022). Inhibition of the vascular endothelial growth factor (VEGF) signaling pathway has emerged as one of the most promising new approaches for cancer therapy. Solid tumors are dependent for growth on nutrients and oxygen they receive via angiogenesis, the process wherein new capillaries are formed from existing blood vessels. This is facilitated by several endogenous proteins among which VEGF α is thought to be key (Folkman 2007). VEGF is secreted by tumors and induces a mitogenic response through its binding to one of three tyrosine kinase receptors (VEGFR-1 to -3) on nearby endothelial cells (Veikkola et al. 2000). Thus inhibition of this signaling pathway should block angiogenesis and subsequent tumor growth (Baka et al. 2006). The first clinical validation of this hypothesis came from bevacizumab, a monoclonal antibody to VEGF, which is approved for the treatment of both metastatic colorectal cancer in combination with 5-fluorouracil, and non-small cell lung cancer in combination with carboplatin and paclitaxel (Ramalingam and Belani 2007). More recently sorafenib and sunitinib, small-molecule multi kinase inhibitors which inhibit the VEGF and platelet-derived growth factor (PDGF) receptor tyrosine kinases among others, have been approved for the treatment of advanced renal-cell carcinoma (Chow and Eckhardt 2007; Kane et al. 2006). The Ochrophyta, *Polycladia myrica* belong to family *Sargassaceae* while *Dictyopteris acrostichoides* belong to family *Dictyotaceae*. *Caulerpa*

racemosa is a Chlorophyta that belongs to the family *Caulerpaceae* and *Halimeda opuntia* belongs to the family *Halimedaceae* (Guiry and Guiry 2022). Family *Dictyotaceae* is considered one of the most important brown algae in the treatment of tumors. *Caulerpa racemosa* provides a dual advantage of better alternative food with therapeutic importance. It has antimicrobial, antiviral, and enzymes inhibitory activities due to the presence of various phytochemicals such as caulerpin, caulerprenylol B, and racemosin A. The algae *Dictyopteris* sp. is an important group of marine seaweeds and is excessively distributed, known by their identified ocean smell due to its secondary metabolites including C₁₁-hydrocarbons and sulfur compounds. *Dictyopteris* has a broad variety of phytoconstituents, covering diterpenes, sesquiterpene, long-chain aliphatic, and acetylenic compounds, which were reported to have antitumor, antimalarial, antibacterial, antifungal, antioxidant, anti-inflammatory, tyrosinase inhibitors, alpha-amylase inhibitors, and small hemolysis activities, *Dictyopteris acrostichoides* has shown a wide range of biological activities, but its phytoconstituents are still elusive (Rushdi et al. 2022). *Halimeda opuntia* is a calcified green algae with antimicrobial, and hepatoprotective activities (Selim 2012). *Polycladia myrica* exhibited antioxidant, antimicrobial, antifungal, and antiviral activity against herpes simplex virus type 1 (HSV-1) (Jassbi et al. 2013).

Thus, the current study characterizes the cytotoxic potential of ethanol extract of four algae including *Caulerpa racemosa*, *Dictyopteris acrostichoides*, *Halimeda opuntia*, and *Polycladia myrica* against HepG2 (human hepatoma), MCF-7 (human breast adenocarcinoma), and Caco-2 (human colon adenocarcinoma) cells assisted by both LC-HR-ESI-MS spectrometry metabolomics and molecular docking analyses to detect the chemical metabolites as well as their possible mode of action.

2. Cells, Materials, and methods

1. Materials and reagents

All used chemicals were of analytical grade and purchased from Sigma (USA), Merck (Germany), and SD Fine Chemicals (India).

2. Algae materials

The seaweed samples (*Caulerpa racemosa*, *Dictyopteris acrostichoides*, *Halimeda opuntia*, and *Polycladia myrica*) were collected in August 2021 from various locations along the coastal region of Hurghada City cost line, Red Sea (27° 17' 01.0"N and 33° 46' 21.0"E), Egypt., and were provided by Prof. Dr. Hashem A. Madkour, department of Marine and Environmental Geology, National Institute of Oceanography and Fisheries, Red Sea Branch, Hurghada, Egypt. The voucher numbers (Da-08/2021, Cr-08/2021, Ho-08/2021, and Pm-08/2021) were deposited in the herbarium unit at the Department of Pharmacognosy, Faculty of Pharmacy, South Valley University, Qena, Egypt.

2.3. Extraction

The samples were collected in sterilized polyethylene bags, and kept in an icebox, for transportation to the laboratory. Samples were rinsed with distilled water (DW) to remove any associated debris. The samples were kept in the Department of Pharmacognosy, Faculty of Pharmacy, South Valley University, Qena, Egypt, and allowed to air dry before being ground to a fine powder. The Air-dried powdered algae materials (200 g) were separately exhaustively extracted with 70% ethanol (600 mL × 3 times). The extracts were then concentrated under reduced pressure at 45°C. The obtained solvent-free residues were stored at 4°C for subsequent analysis. The obtained solvent-free residues (12–28 g) were stored at 4°C for subsequent analysis. 16, 23, 9, and 28 gm are results of crude extracts from *Caulerpa racemosa*, *Dictyopteris acrostichoides*, *Halimeda opuntia*, and *Polycladia myrica* respectively obtained from dry 200gm biomass weights. *Polycladia myrica* yields the highest weight of crude extract (28 g), while calcified algae *Halimeda opuntia* yields the lowest weight (9 g).

3. Screening of cytotoxic activity of ethanol extracts

Cytotoxicity of the ethanol extracts was evaluated in cell lines manipulating the 3-(4,5-dimethylthiazol-2-yl)-2,5-diphenyltetrazolium bromide (MTT) assay (Cheng et al. 2017). MCF-7 (human breast adenocarcinoma), Caco2 (human colon adenocarcinoma), and HepG2 (human hepatoma) cells were preserved in RPMI medium (Merck, Darmstadt, Germany), increased with 10% fetal bovine serum (FBS). Cancer cells were cultivated at 37 °C, 5% (v/v) CO₂ in RPMI1640 medium, supplemented with 1% sodium pyruvate, 1%

(w/v) L-glutamine, 5% (v/v) fetal bovine serum (FBS) and 0.4% (w/v) antibiotics (50 mg/mL streptomycin, 50 U/mL penicillin). Cells were secured from the American Type Culture Collection (ATCC, Rockville, MD, USA; HPACC, Salisbury, UK) and sub-cultivated twice per week. Ethanol extracts were dissolved in DMSO at a concentration of 0.05 g/0.5 mL as a stock solution and filtered to exclude any particles. Further dilutions were made in the culture medium. DMSO used for the detection was of ACS reagent grade from Sigma Aldrich (Darmstadt, Germany). The water used was reverse osmosis water purified using a Millipore cartridge filter. The MTT (3-(4,5-dimethylthiazol-2-yl)-2,5-diphenyltetrazolium bromide) substance and all the other reagents and substances were from commercially (Sigma Aldrich, USA). The glass vials (2 mL) utilized were Fisher-brand with Titeseal closure (Fisher Scientific). To normalize cell viability values, each plate contained a triplicate of cells cured with the various ethanol extracts carrier on DMSO to define 100% viable cells as well as a triplicate of cells incubated with a cytotoxic mixture (25 g/mL CHX (Cycloheximide), 200 ng/mL CD95L (Fas ligand), 200 ng/mL Tumor Necrosis Factor (TNF), 200 ng/mL TRAIL (TNF-related apoptosis-inducing ligand) and 1% (w/v) sodium azide) to detect maximal cell death and thus 0% viability. The viable cells were detected as a dark blue formazan product; no such dark blue staining was detected in the dead cells. All samples were moved to a 96-well plate and absorbance was investigated at 570 nm using a Spectra Max plus Microplate Reader (Molecular Devices, CA, USA). The cell viability is expressed relative to the untreated control cells. All other viability values were normalized to the averages of these triplicates and analyzed by the Graph Pad Prism 5 software (La Jolla, CA, USA), 50%. Doxorubicin was used as a positive control (El-Hawary et al. 2021).

4. Metabolomic profiling of ethanol extract of *Dictyopteris acrostichoides*

Metabolomic profiling of the ethanol extracts of *Dictyopteris acrostichoides* was performed using analytical techniques of liquid chromatography high-resolution Electrospray Ionization Mass Spectrometry (LC-HR-ESI-MS). Detection of the metabolites was performed using ESI MS in both the positive and negative modes. Data were processed and extracted using MZmine2.20. Chromatogram builder and deconvolution followed the detection of mass ion peaks. The local minimum search algorithm was processed, and isotopes were recognized by the isotopic peaks grouper (Attia et al. 2022). An adduct and complex search were done. Then, the processed data set was submitted for peak identification and molecular formula prediction. Both + ve and - ve ionization mode data sets were dereplicated against METLIN and Dictionary of natural products (DNP) databases. Hits from the database were retrieved using Chem-Bio Finder version 13 (Abdel-Rahman et al. 2022).

5. Molecular docking

Molecular modeling and visualization processes were performed within EGFR and VEGFR using Molecular Operating Environment (MOE 2019.0102, 2020; Chemical Computing Group, Montreal, QC, Canada). The co-crystal structure was retrieved from the RCSB Protein Data Bank (PDB code 3UG2 for EGFR and 3CJG for VEGFR). First, compounds were prepared with the standard protocol designated in MOE 2019. The compounds structures energies were minimized using MMF94FX Forcefield with a gradient RMSD of 0.0001 kcal/mol. Then the protein structure was prepared by using the MOE protocol. To validate the docking study at the binding site, the native ligand gefitinib and KIM were re-docked into their binding sites using the same set of parameters as described above. The compounds were then docked after validation in the binding site using the triangle matching placement method. Refinement was carried out using forcefield and scored using the affinity dG scoring system. The resulting docking poses were visually inspected, and the pose of the lowest binding free energy value was considered.

6. The epidermal growth factor receptor (EGFR) kinase assay

5x Kinase assay buffer containing ATP, and 50x PTK substrate. (Optional: If desired, add DTT to 5x Kinase assay buffer to make a 10 mM concentration, e.g., add 10 μ L of 1 M DTT to 1 mL 5x Kinase assay buffer) was used. The master mixture was prepared (25 μ L per well): N wells x (6 μ L 5x Kinase assay buffer + 1 μ L ATP (500 μ M) + 1 μ L 50x PTK substrate + 17 μ L water). 25 μ L was added to every well. 5 μ L of Inhibitor solution was added to each well labeled as "Test Inhibitor". For the "Positive Control" and "Blank", 5 μ L of the same solution without inhibitor (Inhibitor buffer) was added. 3 mL of 1x Kinase assay buffer by mixing 600 μ L of 5x Kinase assay buffer with 2400 μ L water was prepared; 3 mL of 1x Kinase assay buffer is sufficient for 100 reactions. To the wells designated as "Blank", 20 μ L of 1x Kinase assay buffer was added. Thaw EGFR enzyme on ice. Upon the first thaw, a brief tube containing enzyme was spinned to recover the full content of the tube. The amount of EGFR required for the assay was calculated for the dilution of the enzyme to 1 ng/ μ L with 1x Kinase assay buffer. The remaining undiluted enzyme was stored in aliquots at -80°C. Note: EGFR

enzyme is sensitive to freeze/thaw cycles. multiple freeze/thaw cycles were avoided. Thaw aliquots of the diluted enzyme were not re-used. The reaction was initiated by adding 20 μ L of diluted EGFR enzyme to the wells designated "Positive Control" and "Test Inhibitor Control". At 30°C for 40 minutes was incubated. Thaw Kinase-Glo Max reagent. After the 40-minute reaction, 50 μ L of Kinase-Glo Max reagent was added to each well. The plate was covered with aluminum foil and incubated at room temperature for 15 minutes. Luminescence was measured using the microplate reader. All samples and controls were tested in duplicate (Huang et al. 2021).

7. The vascular endothelial growth factor receptor 2 (VEGFR2) kinase assay

5x Kinase Buffer 1 containing ATP, and 50x PTK substrate. (Optional: If desired, add DTT to 5x Kinase Buffer 1 to make a 10 mM concentration, e.g., add 10 μ L of 1 M DTT to 1 mL 5x Kinase Buffer 1) was prepared. The master mixture (25 μ L per well): N wells x (6 μ L 5x Kinase Buffer 1 + 1 μ L ATP (500 μ M) + 1 μ L 50x PTK substrate + 17 μ L water) was prepared. 25 μ L was added to every well. 5 μ L of the inhibitor solution was added to each well labeled as "Test Inhibitor". For the "Positive Control" and "Blank", 5 μ L of the same solution was added without inhibitor (inhibitor buffer). 3 mL of 1x Kinase Buffer 1 was prepared by mixing 600 μ L of 5x Kinase Buffer 1 with 2400 μ L water. 3 mL of 1x Kinase Buffer 1 is sufficient for 100 reactions. For the wells designated as "Blank", add 20 μ L of 1x Kinase Buffer 1. VEGFR2 enzyme on ice was thawed. Upon the first thaw, a brief tube containing enzyme was spined to recover the full content of the tube. The amount of VEGFR2 required for the assay and dilute enzyme to 1 ng/ μ L with 1x Kinase Buffer 1 was calculated. The remaining undiluted enzyme in aliquots was stored at -80°C. Note: VEGFR2 enzyme is sensitive to freeze/thaw cycles. Multiple freeze/thaw cycles were avoided. Thaw aliquots of the diluted enzyme were not re-used. The reaction was initiated by adding 20 μ L of diluted VEGFR2 enzyme to the wells designated "Positive Control" and "Test Inhibitor Control". Incubated at 30°C for 45 minutes Thaw Kinase-Glo Max reagent. After 45 minutes, 50 μ L of Kinase-Glo Max reagent was added to each well. The plate was covered with aluminum foil and incubated at room temperature for 15 minutes. Measuring luminescence by the microplate reader. All samples and controls were tested in duplicate. (Elrazaz et al. 2021).

3. Results

1. Cytotoxic activity

The obtained results revealed that the ethanol extract of *Dictyopteris acrostichoides* had promising cytotoxicity activities against HepG2, MCF-7, and Caco-2 cell lines with IC_{50} values of 11.65, 9.28, and 16.86 μ g/mL, respectively compared to doxorubicin (IC_{50} = 5.72, 5.17 and 5.81 μ g/mL, respectively), thus, it was further subjected to other assays while other extracts of *Caulerpa racemose*, *Halimeda opuntia* and *Polycladia myrica* did not show cytotoxic activities against tested cell lines.

2. LC_MS analysis of ethanol extract of

2. LC_MS analysis of ethanol extract of *Dictyopteris acrostichoides*

LC-HR-MS analysis (Fig. 1) for dereplication purposes was adopted for the identification of metabolites from ethanol extract of *Dictyopteris acrostichoides* (Table 1, Fig. 2). The dereplication study of the metabolites against the DNP (Dictionary of natural products) and MarinLit databases resulted in the identification of 17 compounds.

Table 1
Dereplicated compounds from *Dictyopteris acrostichoides* extract

NO.	Mode	m/z	Mw	Molecular formula	Dereplication	Class	Source	References
1	P	221.1906	220.1833	C ₁₅ H ₂₄ O	α-Dictyopterol ^a	Sesquiterpene	<i>D. divaricate</i>	(Etsuro et al. 1966)
2	P	221.1906	220.1833	C ₁₅ H ₂₄ O	β-Dictyopterol ^a	Sesquiterpene	<i>D. divaricate</i>	(Etsuro et al. 1966)
3	P	221.1906	220.1833	C ₁₅ H ₂₄ O	Germacra-1(10),4(15)-11-trien-5S-ol ^a	Sesquiterpene	<i>D. divaricate</i>	(Toshi et al. 1964)
4	N	255.1967	256.204	C ₁₅ H ₂₈ O ₃	4α,5β-Dihydroxycubanol ^a	Sesquiterpene	<i>D. divaricate</i>	(Qiao et al. 2009)
5	N	255.1967	256.204	C ₁₅ H ₂₈ O ₃	Cadinan-1,4,5-triol ^a	Sesquiterpene	<i>D. divaricate</i>	(Qiao et al. 2009)
6	N	303.2325	304.2397	C ₂₀ H ₃₂ O ₂	(1 <i>R</i> ,3 <i>R</i> ,4 <i>S</i> ,11 <i>R</i>)-3,4,7,8-Bisepoxydolabellan-12(18)-ene ^a	Sesquiterpene	<i>D. delicatula</i>	(Wright et al. 1990)
7	P	313.2157	312.2085	C ₂₁ H ₂₈ O ₂	Chromenol ^a	Sesquiterpene	<i>D. undulate</i>	(Wang et al. 2018)
8	P	313.2157	312.2085	C ₂₁ H ₂₈ O ₂	Dictyochromenol ^a	Sesquiterpene	<i>D. undulate</i>	(Li et al. 2022)
9	P	313.2157	312.2085	C ₂₁ H ₂₈ O ₂	Isochromazonarol ^a	Sesquiterpene	<i>D. undulata</i>	(Ishibashi et al. 2013)
10	P	315.2327	314.2254	C ₂₁ H ₃₀ O ₂	Chromazonarol ^a	Sesquiterpene	<i>D. undulate</i>	(Ishibashi et al. 2013)
11	P	315.2327	314.2254	C ₂₁ H ₃₀ O ₂	Isozonarol ^a	Hydroquinone	<i>D. zonarioides</i>	(Fenical et al. 1973)
12	P	315.2327	314.2254	C ₂₁ H ₃₀ O ₂	Zonarol ^a	Hydroquinone	<i>D. zonarioides</i>	(Fenical et al. 1973)
13	P	315.2327		C ₂₁ H ₃₀ O ₂	2-[(2 <i>E</i> ,6 <i>E</i>)-3,7,11-Trimethyldodeca-2,6,10-trien-1-yl]benzene-1,4-diol ^a	Sesquiterpene	<i>D. undulate</i>	(Ishibashi et al. 2013)
14	P	343.2257	342.2184	C ₂₂ H ₃₀ O ₃	Zonaric acid ^a	Sesquiterpene	<i>D. undulate</i>	(Ishibashi et al. 2013)
15	P	361.2366	360.231	C ₂₂ H ₃₂ O ₄	Dictyvaric acid ^a	Sesquiterpene	<i>D. divaricata</i>	(Song et al. 2005)
16	N	401.2536	402.2609	C ₂₂ H ₄₂ O ₂ S ₂	1-(3-Oxo-undecyl)disulfanyl)-undecan-3-one ^a	Disulfide	<i>D. plagiogramma</i>	(Schnitzler et al. 1998)
17	N	485.2762	486.2835	C ₂₆ H ₄₆ O ₄ S ₂	Di(3-acetoxy-5-undecenyl) disulfide ^a	Disulfide	<i>Dictyopteris sp.</i>	(Moore et al. 1972)

^a Compound identified for the first time from *Dictyopteris acrostichoides* but previously identified from genus *Dictyopteris*.

3. Molecular docking

Molecular docking simulation of compounds (**1–17**), **Gefitinib**, or **KIM** into the corresponding active sites was done. They got stabilized at the binding sites by variable several electrostatic bonds. All compounds showed nearly binding interactions like gefitinib or KIM as rmsd-refine were less than 2 Å (Tables 2, 3). (Fig. 3–8). The docking on the EGFR showed that all the target compounds (**1–17**) could interact with the active sites of the co-crystallized ligand binding sites (Hu et al. 2017). Also, most compounds showed hydrogen bonding with the gatekeeper mutant Met790. Interestingly, compounds 17 and 16 showed higher docking scores than **Gefitinib** (Table 2, Fig. 3–5). Compounds (**2, 5, 8–15**) were of good binding energies ranging from – 6.9734 to –6.1317 kcal/mol. While (**1, 3–4, 6–7**) were of fair binding energies less than 6 kcal/mol. The docking on VEGFR revealed that Most compounds formed hydrogen bonding with Asp 1044 like that of the ligand KIM. Compound (**17**) has a binding score (–8.2601 kcal/mol) more than ligand **KIM** (–7.8176 kcal/mol) while compounds (**16**) and (**12**) showed – 7.4368 and – 7.0233 kcal/mol, respectively (Table 3, Fig. 6–8). Compounds (**8–11, 13–15**) showed good binding energies ranging from – 6.8160 to –6.3920 kcal/mol. Most compounds formed hydrogen bonding with Asp 1044 like that of the ligand **KIM**.

3.1. Target compounds optimization

The target compounds were constructed into a 3D model. After checking their structures and the formal charges on atoms by the 2D depiction, the following steps were carried out: The target compounds were subjected to a conformational search. All conformers were subjected to energy minimization, and all the minimizations were performed until an RMSD gradient of 0.01 Kcal/mole and RMS distance of 0.1 Å with MMFF94X force-field, and the partial charges were automatically calculated. The obtained database was then saved as an MDB file to be used in the docking calculations.

3.2. Optimization of the enzyme active site

The X-ray crystallographic structure of EGFR and VEGFR complexed with **Gefitinib** and **KIM**, respectively, were obtained from the Protein Data Bank through the internet (<http://www.rcsb.org/>, PDB code 3UG2 for EGFR [50] and 3CJG for VEGFR). The protein was prepared for docking studies by Hydrogen atoms were added to the system with their standard geometry. The atoms connection and type were checked for any errors with automatic correction. The selection of the receptor and its atoms potential were fixed. Site Finder was used for the active site search in the enzyme structure using all default items. Dummy atoms were created from the site finder of the pocket.

Table 2
 Receptor interaction of compounds (1–17) and **gefitinib** into the gefitinib binding site in EGFR (PDB: 3UG2)

Compound	S	E_conf	rmsd_refine	Receptor
	dG Kcal/mole	Kcal/mole		Amino acid/Type of bonding/Distance (Å) / Binding Energy (Kcal/mole)
1	-5.8597	19.9494	1.2122	MET 790/H-donor/4.47/-0.2
2	-6.1317	5.4980	1.7807	MET 790/H-donor/4.44/-0.6 LYS 745/H-acceptor/3.05/-5.4 PHE 723/H-pi/3.92/-0.5
3	-5.5341	-1.5846	1.3102	MET 790/H-donor/3.71/-0.8
4	-5.9620	11.3812	1.1552	MET 790/H-donor/3.52/-0.4 LYS 745/H-acceptor/2.93/-0.9
5	-6.3042	25.7398	1.9793	MET 790/H-donor/3.97/-0.3 THR 854/H-donor/2.90/-1.1 MET 790/H-donor/3.59/-0.4 MET 790/H-donor/3.63/-0.3 ASP 855/H-acceptor/2.95/-0.8 THR 854/H-acceptor/2.76/-0.2
6	-5.8232	311.1455	1.1227	MET 790/H-donor/4.36/-0.2 MET 790/H-donor/4.12/-0.3 ALA 743/H-acceptor/3.23/-0.2
7	-4.4723	-17.4830	1.7636	GLU 762/H-donor/2.85/-3.5 LEU 844/pi-H/4.60/-0.3
8	-6.5644	-23.9966	1.8709	GLN 791/H-donor/3.16/-0.3 GLN 791/H-donor/2.91/-2.8 PHE 723/H-pi/4.14/-0.2
9	-6.2402	50.5312	0.8622	MET 790/H-donor/3.47/-0.6 MET 790/H-donor/3.99/-0.2 PHE 723/H-pi/4.32/-0.4
10	-6.8688	10.4155	1.5001	ASP 855/H-donor/3.08/-1.3 MET 790/H-donor/4.18/-0.2 LYS 745/pi-H/4.09/-0.3 MET 766/pi-H/4.50/-0.2
11	-6.6728	2.5902	1.2996	MET 790/H-donor/3.58/-0.2 MET 790/H-donor/4.02/-0.2 MET 790/H-donor/4.42/-0.2 VAL 726/pi-H/4.69/-0.3

Compound	S	E_conf	rmsd_refine	Receptor
	dG Kcal/mole	Kcal/mole		Amino acid/Type of bonding/Distance (Å) / Binding Energy (Kcal/mole)
12	-6.5444	12.7228	0.8959	GLU 762/H-donor/3.10/-0.3 ASP 855/pi-H/4.79/-0.3
13	-6.9734	-16.9074	1.9808	GLU 762/H-donor/2.84/-3.1 MET 790/H-donor/3.69/-0.2 CYS 797/H-donor/3.86/-0.2 PHE 723/H-pi/4.41/-0.3 LYS 745/pi-H/4.79/-0.2 LYS 745/pi-cation/4.07/-0.2 MET 766/pi-H/4.39/-0.3 ASP 855/pi-H/4.51/-0.2
14	-6.7161	-18.2702	1.8968	CYS 797/H-donor/4.20/-0.2 LYS 745/pi-H/4.88/-0.4
15	-6.9689	-61.6212	1.7331	MET 790/H-donor/4.35/-0.2 MET 790/H-donor/3.47/-1.3 GLU 762/H-donor/3.55/-0.2 LYS 745/H-acceptor/2.86/-5.0 LYS 745/Ionic/2.86/-5.5 LYS 745/pi-cation/3.85/-0.5
16	-7.9106	-4.4830	1.5842	MET 790/H-donor/4.28/-0.2 LYS 745/H-acceptor/4.05/-0.2 LYS 745/H-acceptor/3.87/-0.2 VAL 726/H-acceptor/4.38/-0.2 VAL 726/H-acceptor/3.94/-0.2 ASP 855/H-acceptor/3.14/-0.4
17	-8.2612	-44.4652	1.7402	VAL 726/H-acceptor/4.35/-0.2 VAL 726/H-acceptor/4.04/-0.3 LEU 844/H-acceptor/4.23/-0.2 LEU 844/H-acceptor/3.98/-0.2

Compound	S	E_conf	rmsd_refine	Receptor
	dG	Kcal/mole		Amino acid/Type of bonding/Distance (Å) / Binding Energy (Kcal/mole)
	Kcal/mole			
Gefitinib	-7.4119	3.1893	1.4770	ASP 855/H-donor /3.13/ -0.2
				MET 790/H-donor/4.29/-0.4
				ASP 855/H-donor/3.47/ -1.7
				PHE 723/pi-H/ 3.86/-0.2
				MET 766/pi-H/4.86/-0.3
				ARG 841 /pi-H/4.61/-0.4
				THR 854/pi-H/3.76/-0.4
				THR 854/ pi-H/4.08/-0.2

Table 3
 Receptor interaction of compounds (1–17) and ligand (KIM) into the ligand (KIM) binding site in VEGFR (PDB: 3CJG).

Compound	S	E_conf	rmsd_refine	Receptor
	dG Kcal/mole	Kcal/mole		Amino acid/Type of bonding/Distance (Å) / Binding Energy (Kcal/mole)
1	-5.9916	19.2320	0.7421	GLU 883/H-donor/2.66/-3.3
2	-5.5544	8.5498	0.94640	CYS 1043/H-donor/4.01/ -0.2 LYS 866/H-acceptor/3.11/-5.1
3	-5.2952	-3.0075	1.7793	LYS 866/ H-acceptor/3.36/-2.3
4	-5.2926	7.8920	1.2934	CYS 1043/H-donor /3.98/ -0.2 ASP 1044/H-donor/3.21/-1.1 ASP 1044/H-donor/3.29/-0.2 ASP 1044/H-donor/2.93/-2.1 ARG 840/H-acceptor/3.37/-1.4
5	-5.9565	30.6141	1.14360	GLU 883/H-donor/3.16/-1.0 LYS 866/H-acceptor/2.93/-5.8 LYS 866/H-acceptor/2.94/-0.4
6	-5.7807	300.1895	2.0049	LYS 866/H-acceptor/3.06/-3.5
7	-4.5827	-17.5563	1.5359	LEU 838/pi-H/4.12/-0.5 LEU 838/pi-H/4.23/-0.3 LEU 838/pi-H/ 4.04/-0.7
8	-6.6525	-26.3838	1.4419	LEU 1033/pi-H/4.05/-0.2
9	-6.6549	38.3437	1.7441	ASP 1044/H-donor/3.26/-0.2
10	-6.4106	8.41960	2.0775	LEU 838/pi-H/4.74/-0.2
11	-6.3920	2.9560	1.3160	CYS 1043/H-donor/4.11/-0.2
12	-7.0233	13.5903	1.4213	GLU 915/H-donor/3.09/-0.9 CYS 917/H-acceptor/2.89/-1.3 LEU 838/pi-H/4.33/-0.4 VAL 846/pi-H/4.44/-0.2
13	-6.6623	-26.8596	1.8448	PHE 843/H-donor/2.97/-3.0 ARG 840/pi-H/ 3.64/-0.4
14	-6.5834	-10.5786	1.3041	GLY 839/H-donor/3.55/-0.2 LYS 866/H-acceptor/2.97/-2.1 LYS 866/Ionic/2.97/-4.7 ARG 840/Ionic/3.13/-3.7 ARG 840/pi-H/3.93/-0.2 ARG 840/pi-cation/4.50/-1.4

Compound	S	E_conf	rmsd_refine	Receptor
	dG Kcal/mole	Kcal/mole		Amino acid/Type of bonding/Distance (Å) / Binding Energy (Kcal/mole)
15	-6.8160	1.7617	-63.6101	ASP 1044/H-donor/3.55/-0.2
				CYS 1043/H-donor/3.03/-0.2
				GLY 1046/H-acceptor/3.83/-0.2
				ASP 1044/H-acceptor/3.06/-0.5
				ARG 840/pi-H/4.49/-0.2
				LYS 866/pi-cation/3.52/-0.2
16	-7.4368	4.1228	1.5586	ASP 1044/H-acceptor/3.59/-0.9
				ASP 1044/H-acceptor/3.51/-0.5
				ASP 1044/H-acceptor/3.67/-0.6
				PHE 1045/H-acceptor/3.76/-0.5
				GLY 1046/H-acceptor/4.49/-0.5
17	-8.2601	-36.7409	1.4837	VAL 846/H-acceptor/3.92/-0.2
Ligand KIM	-7.8176	-90.5341	1.7030	GLY 841/H-donor/3.61/-0.3
				ASP 1044/H-donor/3.06/-0.4
				ASP 1044/H-donor/3.37/-0.3
				LYS 866/H-acceptor/3.02/-6.0
				LEU 838/pi-H/4.50/-0.4
				LEU 838/pi-H/4.49/-0.2
				ARG 840/pi-H/4.79/-0.2
				VAL 846/pi-H/4.50/-0.4
				VAL 846/pi-H/4.45/-0.4
LYS 866/pi-H/3.82/-0.2				

4. EGFR and VEGF activities

Further screen of ethanol extract of *Dictyopteris acrostichoides* displayed in vitro activity against epidermal growth factor receptor (EGFR) kinase ($IC_{50} = 0.11 \mu\text{g/mL}$) compared to Lapatinib as a positive control ($IC_{50} = 0.03 \pm 0.002 \mu\text{g/mL}$) and against vascular endothelial growth factor (VEGF) ($IC_{50} = 0.276 \mu\text{g/mL}$) compared to Sorafenib as a positive control ($IC_{50} = 0.049 \pm 0.003 \mu\text{g/mL}$).

5. Discussion

Cancer is one of the top causes of mortality worldwide. More than half of all cancer deaths each year are caused by lung, colorectal, liver, and stomach cancers (Kumara et al. 2017). Many biomarkers like Epidermal Cyclooxygenase-2 (COX-2), Phosphoinositide 3-kinase (PI3k), Growth Factor Receptor (EGFR), Nuclear factor-kappa β (NF- κ β), and Activator protein (AP-1) are expressed in various types of cancer. EGFR overexpression is thought to play an important role in the activation of various malignant tumors. The epidermal growth factor receptor (EGFR) is considered a receptor tyrosine kinase of the ErbB family that is abnormally activated in many epithelial tumors. Two classes of anti-EGFR agents have currently approved for treatment of patients with cancer: cetuximab, a monoclonal antibody directed at the extracellular domain of the receptor, and gefitinib and erlotinib, oral, low-molecular-weight (MW), adenosine triphosphate (ATP)-competitive inhibitors of the receptor's tyrosine kinase (Mendelsohn and Baselga 2006). EGFR stimulates tumor growth and progression through several mechanisms, namely angiogenesis, promoting proliferation, invasion,

metastasis, and differentiation, inhibiting apoptosis, and adhesion. Therefore, EGFR is a rational target for antitumor strategies.6. The expression of transcription, mutation, and/or gene amplification may be the cause of EGFR activation in tumor cells. The increased protein and transcribed levels of EGFR will correspond to poor prognosis in several cancers such as lung cancer and colorectal cancer (Zakaria et al. 2019). The VEGFR has multiple immediate effects on cancer cells and is known to have a major contribution to angiogenesis aims to abolish the nutrient and oxygen supply to the tumor cells through the decrease of the vascular network and the avoidance of new blood vessel formation. In vitro experiments on capillary endothelial cells have shown that VEGFR is a potential stimulator of angiogenesis because its presence as a growth factor causes endothelial cell proliferation migration, and tube formation in capillary junctions (Pauty et al. 2018). Stimulation of VEGFR signaling could enhance cancer cell growth by being involved in the angiogenesis process which requires solid tumor growth (Lopes-Coelho et al. 2021). Delile is a sesquiterpene lactone from *Vernonia amygdalina* considered a new anticancer potential on the expression of cancer therapeutic target: epidermal growth factor receptor (EGFR), and vascular endothelial growth factor receptor (VEGFR) (Nerdy et al. 2022). Ethanol extract of *Dictyopteris acrostichoides* was tested for cytotoxicity activities against HepG2 (human hepatoma), MCF-7 (human breast adenocarcinoma), and CACO-2 (human colon adenocarcinoma) cells (IC₅₀ = 11.65, 9.28 and 16.86 µg/mL, respectively). Ethanol extract of *D. acrostichoides* has inhibitory effect on epidermal growth factor receptor (EGFR) kinase (IC₅₀ = 0.11 µg/mL) and the vascular endothelial growth factor (VEGF) (IC₅₀ = 0.276 µg/mL). The methanol extracts of *D. delicatula* and *D. australis* collected from Natal (Brazil), were reported as antioxidants and showed very high DPPH radical scavenging activity (IC₅₀ = 0.66 ± 0.002 and 1.60 ± 0.013 mg/mL, respectively) due to the total phenolic content (21.34 ± 0.428 and 13.19 ± 0.32 GAE mg/g of total methanol extract, severally). Dose-dependent cytotoxic activities were detected against the brine shrimp *A. salina*. The highest cytotoxic activity of *D. australis* was at a dose of 100 µg/mL in 18 and 24 hs and caused complete mortality of the brine shrimp at a dose of 500 µg/mL in 24 hs (Vinayak et al. 2011). The ethyl acetat fraction of *D. divaricata* have cytotoxic activities against the B16F10 (murine melanoma cells), HT-29 (human colon carcinoma), HL-60 (human promyelocytic leukemia) and A549 (human lung cancer cell lines) due to cell shrinkage, cell membrane blebbing and formation of apoptotic bodies (Kim et al. 2009). The ethanol extract of *D. prolifera*, collected from Korea, evaluated for its inhibitory effects on α-glucosidase. It showed effective inhibitory activity (99.2%, IC₅₀ = 16.66 µg/mL) compared to a positive control (Acarbose, 70.3%), with no cytotoxicity on 3T3-L1 (Jeong et al. 2012). Polysaccharides in *D. delicatula*, collected from Brazil, were detected to have a dose-dependent antioxidant activity and suppress cervical cancer cell lines (HeLa) proliferation. The percentage of inhibition ratio was calculated for antiproliferative activity (61.0%, 2 mg/mL). The antiproliferative efficacy of these polysaccharides was related to the sulfate content (Costa et al. 2010). The hexane extract of *D. divaricata* collected from China had strong cytotoxic activities against ubiquitous keratin-forming tumor cells (IC₅₀ < 4.40 µg/mL) (Xu et al. 2004). Twelve metabolites such as dimethyl 2,6-dibromoterephthalate were isolated from the methanol extract of *D. hoytii* and were evaluated for in vitro bovine carbonic anhydrase-II (CA-II) inhibitory activity and exhibited significant inhibitory activity against CA-II with IC₅₀ values ranging from 13.4 to 71.6 µM (Rafiq et al. 2021). The *D. undulata* ethanol extract have cytotoxic potential against SW480, SNU407 and HT29 cells with 50% inhibition of cell viability at a concentration of 40 µg/mL in a dose-dependent manner. *D. undulata* ethanol extract induced programmed cell death in SW480 cells due to apoptotic body formation, DNA fragmentation, an increase in the population of apoptotic sub-G1 phase cells, and mitochondrial membrane depolarization, significantly modulated the expression of apoptosis associated proteins, resulting in a decrease in B cell lymphoma-2 expression and an increase in Bcl-2-associated X protein expression, as well as the activation of caspase-9 and caspase-3 (Kim et al. 2014). Cadinan-1,4,5-triol (**5**) was detected in *D. divaricata* extract and was inactive against several human cancer cell lines including stomach cancer (BGC-823), lung adenocarcinoma (A549), hepatoma (Bel7402), breast cancer (MCF-7), and colon cancer (HCT-8) cell lines (Song et al. 2004). Dictyochromenol (**8**) had antiplasmodial activity (*P. falciparum* strain FCB-1, IC₅₀ = 9.58 µg/mL) with cytotoxicity to rat skeletal muscle myoblast (L-6 cells, IC₅₀ = 7.71 µg/mL) (Vega et al. 2008). Isochromazonarol (**9**), chromazonarol (**10**), 2-[(2E,6E)-3,7,11-trimethyldodeca-2,6,10-trien-1-yl] benzene-1,4-diol (**13**), and zonaric acid (**14**), were isolated from methanol extract of *D. undulata*. The algicidal activity of the isolated compounds was reported against red tide microalgal species (Ishibashi et al. 2013). The bioassay-guided of the selected marine seaweed ethanol extract of *D. acrostichoides* as a source of bioactive natural products, resulted in the detection of (3-Oxo-undecyldisulfanyl)-undecan-3-one (**16**) and di(3-acetoxy-5-undecenyl) disulfide (**17**) along with fifteen known metabolites α-dictyopterol (**1**), β-dictyopterol (**2**), germacra-1(10),4(15)-11-trien-5S-ol (**3**), 4α,5β-dihydroxycubenol (**4**), cadinan-1,4,5-triol (**5**), (1R,3R,4S,11R)-3,4;7,8-bisepoxydolabellan-12(18)-ene (**6**), chromenol (**7**), dictyochromenol (**8**), isochromazonarol (**9**), chromazonarol (**10**), isozonarol (**11**), zonarol (**12**), 2-[(2E,6E)-3,7,11-trimethyldodeca-2,6,10-trien-1-yl] benzene-1,4-diol (**13**), zonaric acid (**14**), and dictyvaric acid (**15**) from LC-HR-ESI-MS metabolic profiling of the ethanol extract of *D. acrostichoides*. Based on molecular docking simulation on those binding sites 1-(3-Oxo-undecyldisulfanyl)-undecan-3-one (**16**) and di(3-acetoxy-5-undecenyl) disulfide (**17**) showed acceptable interaction energies and formed significant interactions EGFR and VEGF binding sites. The docking on the EGFR showed that all the target compounds (**1–17**)

could interact with the active sites of the co-crystallized ligand binding sites. Also, most compounds showed hydrogen bonding with the gatekeeper mutant Met790. Interestingly, compounds **(16)** and **(17)** showed higher docking scores than gefitinib. Compounds **(2, 5, 8–15)** and were of good binding energies ranging from -6.9734 to -6.1317 kcal/mol While **(1, 3–4, 6–7)** were of fair binding energies less than 6 kcal/mol. The docking on VEGFR revealed that Most compounds formed hydrogen bonding with Asp 1044 like that of the ligand KIM. Di(3-acetoxy-5-undecenyl) disulfide **(17)** has a binding score (-8.2601 kcal/mol) more than ligand KIM (-7.8176 kcal/mol) while compounds **(16,12)** showed -7.4368 and -7.0233 kcal/mol, respectively. Compounds **(8–11,13, 14–15)** showed good binding energies ranging from -6.8160 to -6.3920 kcal/mol. Most compounds formed hydrogen bonding with Asp 1044 like that of the ligand KIM.

6. Conclusions

Malignancy is a major threat with severe symptoms worldwide. Finding out a natural drug that inhibits epidermal growth factor receptor (EGFR) kinase and vascular endothelial growth factor (VEGF) will result in a pivotal role in controlling its replication and transcription. Our results demonstrated that *Dictyopteris acrostichoides* ethanol extract displayed cytotoxicity against HepG2, MCF-7 and CACO-2 ($IC_{50} = 11.65, 9.28$ and 16.86 $\mu\text{g/mL}$, respectively) compared to doxorubicin as a positive control, ($IC_{50} = 5.72, 5.17$ and 5.81 $\mu\text{g/mL}$, respectively). Furthermore, the ethanol extract of *D. acrostichoides* was tested against epidermal growth factor receptor (EGFR) kinase ($IC_{50} = 0.11$ $\mu\text{g/mL}$) compared to lapatinib as a positive control, ($IC_{50} = 0.03$ $\mu\text{g/mL}$) and against vascular endothelial growth factor (VEGF) ($IC_{50} = 0.276$ $\mu\text{g/mL}$) compared to sorafenib as a positive control, ($IC_{50} = 0.049$ $\mu\text{g/mL}$). Seventeen metabolites were identified from the ethanol extract of *Dictyopteris acrostichoides* but were detected using LC-HR-ESI-MS for dereplication purposes. To the best of our knowledge, this is the first comprehensive report on the detection of biologically active secondary metabolites from *Dictyopteris acrostichoides*. All detected metabolites were reported herein for the first time from *D. acrostichoides* but were detected before in the genus *Dictyopteris*. The relationship between the identified compounds and interactions with EGFR and VEGF binding site in the cancer cell receptors were studied. Interestingly, 1-(3-oxo-undecylsulfanyl)-undecan-3-one **(16)** confirmed considerable interaction energies and formed substantial interactions EGFR binding site. Interestingly, di(3-acetoxy-5-undecenyl) disulfide **(17)** confirmed considerable interaction energies and formed substantial interactions VEGFR binding site. This study will provide a basis for the search for an alternative source of therapeutic agents from *Dictyopteris acrostichoides*, which can in turn be used as lead candidates for future drug development as new cytotoxic agents.

Declarations

Acknowledgments

We would like to thank South Valley University for supporting this work.

Ethical Approval

In this study, animal experiments were not applicable. All procedures involving human cell lines were approved by the South Valley University Research Ethics Committee (reference P.S.V.U 149).

Consent to Publish

Not applicable.

Declaration of Competing Interest.

The authors declare that they have no conflict of interest.

Funding

This research did not receive any specific grant from funding agencies in the public, commercial, or not-for-profit sectors.

Author Contribution Statement

U.R. was involved in the conceptualization, and supervision of project administration. E.Z.A, M.I.R, I.A.M.A and H.S were responsible for methodology, investigation, resources, data curation, and writing the original draft manuscript. E.Z.A. and M.I.R were involved in

data curation and visualization. E.Z.A., M.I.R, O.M.A. and U.R.A were responsible for software, validation, formal analysis, writing, editing, and reviewing the manuscript.

References

1. Abdel-Rahman IAM, Attia EZ, Aly OM, Saber H, Rushdi MI, Abdelmohsen UR (2022) Metabolite profiling of green algae *Halimeda opuntia* to target hepatitis C virus-796 polymerase inhibitors assisted by molecular docking S. Afr J Bot 151:538–543. <https://doi.org/10.1016/j.sajb.2022.10.038>
2. Allam HA, Aly EE, Farouk AKB, El Kerdawy AM, Rashwan E, Abbass SES (2020) Design and synthesis of some new 2,4,6-trisubstituted quinazoline EGFR inhibitors as targeted anticancer agents. Bioorg Chem 98:103726. <https://doi.org/10.1016/j.bioorg.2020.103726>
3. Attia EZ, Youssef NH, Saber H, Rushdi MI, Abdel-Rahman IAM, Darwish AG, Abdelmohsen UR (2022) *Halimeda opuntia* and *Padina pavonica* extracts improve growth and metabolic activities in maize under soil-saline conditions. J Appl Phycol. 10.1007/s10811-022-02844-6
4. Baka S, Clamp AR, Jayson GC (2006) A review of the latest clinical compounds to inhibit VEGF in pathological angiogenesis Expert Opin. Ther Targets 10:867–876. <https://doi.org/10.1517/14728222.10.6.867>
5. Cheng C, Othman EM, Stopper H, Edrada-Ebel R, Hentschel U, Abdelmohsen UR (2017) Isolation of Petrocidin A, a new cytotoxic cyclic dipeptide from the marine sponge-derived Bacterium *Streptomyces* sp. SBT348. Mar Drugs 15. doi:10.3390/md15120383
6. Chow LQ, Eckhardt SG (2007) Sunitinib: from rational design to clinical efficacy. J Clin Oncol 25:884–896. 10.1200/JCO.2006.06.3602
7. Costa LS et al (2010) Biological activities of sulfated polysaccharides from tropical seaweeds. Biomed Pharmacother 64:21–28. <https://doi.org/10.1016/j.biopha.2009.03.005>
8. El-Hawary SS et al (2021) Cytotoxic activity and metabolic profiling of fifteen. Euphorbia Species Metabolites 11:15. <https://doi.org/10.3390/metabo11010015>
9. Elrazaz EZ, Serya RAT, Ismail NSM, Albohy A, Abou El Ella DA, Abouzid KAM (2021) Discovery of potent thieno[2,3-d]pyrimidine VEGFR-2 inhibitors: Design, synthesis and enzyme inhibitory evaluation supported by molecular dynamics simulations. Bioorg Chem 113:105019. <https://doi.org/10.1016/j.bioorg.2021.105019>
10. Etsuro K, Motowo I, Koji Y, Tadashi M, Toshi I (1966) Sesquiterpenes from *Dictyopteris divaricata*. II dictyopterol and dictyopterone Bull Chem Soc Jpn 39:2509–2512. 10.1246/bcsj.39.2509
11. Fenical W, Sims JJ, Sqatrio D, Wing RM, Radlick P (1973) Zonarol and isozonarol, fungitoxic hydroquinones from the brown seaweed *Dictyopteris zonarioides*. J Org Chem 38:2383–2386. 10.1021/jo00953a022
12. Folkman J (2007) Angiogenesis: an organizing principle for drug discovery? Nat Rev Drug Discov 6:273–286. <https://doi.org/10.1038/nrd2115>
13. Guiry M, Guiry G (2022) AlgaeBase. World-wide electronic publication. National University of Ireland <https://www.algaebase.org/>
14. Hassan A, Badr M, Abdelhamid D, Hassan HA, Abourehab MAS, Abuo-Rahma GEDA (2022) Design, synthesis, in vitro antiproliferative evaluation and in silico studies of new VEGFR-2 inhibitors based on 4-piperazinylquinolin-2(1H)-one. scaffold Bioorg Chem 120:105631. <https://doi.org/10.1016/j.bioorg.2022.105631>
15. Hu C et al (2017) Discovery and characterization of a novel irreversible EGFR mutants selective and potent kinase inhibitor CHMFL-EGFR-26 with a distinct. binding mode Oncotarget 8:18359. 10.18632/oncotarget.15443
16. Huang W, Xing Y, Zhu L, Zhuo J, Cai M (2021) Sorafenib derivatives-functionalized gold nanoparticles confer protection against tumor angiogenesis and proliferation via suppression of EGFR and VEGFR-2. Exp Cell Res 406:112633. <https://doi.org/10.1016/j.yexcr.2021.112633>
17. Ishibashi F, Sato S, Sakai K, Hirao S, Kuwano K (2013) Algicidal sesquiterpene hydroquinones from the brown alga *Dictyopteris undulata*. Biosci Biotechnol Biochem 77:1120–1122. <https://doi.org/10.1271/bbb.130018>
18. Jassbi AR, Mohabati M, Eslami S, Sohrabipour J, Miri R (2013) Biological activity and chemical constituents of red and brown algae from the Persian Gulf Iran. J Pharm Res 12:339
19. Jeong S-Y, Qian Z-J, Jin Y-J, Kim G-O, Yun P-Y, Cho T-OJNPS (2012) Investigation of alpha-glucosidase inhibitory activity of ethanolic extracts from 19 species of marine macroalgae in Korea. Nat Prod Sci 18:130–136

20. Kane RC et al (2006) Sorafenib for the treatment of advanced renal cell carcinoma. *Clin Cancer Res* 12:7271–7278. <https://doi.org/10.1158/1078-0432.CCR-06-1249>
21. Kim AD et al (2014) Dictyopteris undulata extract induces apoptosis in human colon cancer cells. *Biotechnol Bioprocess Eng* 19:419–425. doi:10.1007/s12257-014-0200-8
22. Kim K et al (2009) In vitro cytotoxic activity of *Sargassum thunbergii* and *Dictyopteris divaricata* (Jeju seaweeds) on the HL-60 tumour cell line. *Int J Pharmacol* 5:298–306. 10.3923/lip.2009.298.306
23. Kumara M, Shylajab M, Nazeem P, Babu T (2017) 6-Gingerol is the most potent anticancerous compound in ginger (*Zingiber officinale* Rosc). *J Dev Drugs* 6:1–6. 10.4172/2329-6631.1000167
24. Li H-Y et al (2022) Antibacterial and antifungal sesquiterpenoids: chemistry, resource, and activity. *Biomol Ther* 12:1271. <https://doi.org/10.3390/biom12091271>
25. Lopes-Coelho F, Martins F, Pereira SA, Serpa J (2021) Anti-angiogenic therapy: current challenges and future perspectives. *Int J Mol Sci* 22:3765. <https://doi.org/10.3390/ijms22073765>
26. Mendelsohn J, Baselga J (2006) Epidermal growth factor receptor targeting. in *cancer Semin Oncol* 33:369–385. <https://doi.org/10.1053/j.seminoncol.2006.04.003>
27. Moore RE, Mistysyn J, Pettus JA (1972) (-)-Bis-(3-acetoxyundec-5-enyl) disulphide and S-(-)-3-acetoxyundec-5-enyl thioacetate, possible precursors to undeca-1,3,5-trienes in Dictyopteris. *J Chem Soc Chem Commun* 326–327. 10.1039/C39720000326
28. Nerdy N, Lestari P, Fahdi F, Putra E, Amir S, Yusuf F, Bakri T (2022) In silico studies of sesquiterpene lactones from *Vernonia amygdalina* delile on the expression of EGFR and VEGFR as a new anticancer potential. *Pharmacogn J* 14.13. 10.5530/pj.2022.14.13
29. Pauty J et al (2018) A vascular endothelial growth factor-dependent sprouting angiogenesis assay based on an in vitro human blood vessel model for the study of anti-angiogenic drugs *EBioMedicine*. 27:225–236. <https://doi.org/10.1016/j.ebiom.2017.12.014>
30. Qiao Y-Y, Ji N-Y, Wen W, Yin X-L, Xue Q-Z (2009) A new epoxy-cadinane sesquiterpene from the marine brown alga Dictyopteris divaricata. *Mar Drugs* 7:600–604. <https://doi.org/10.3390/md7040600>
31. Rafiq K et al (2021) New Carbonic anhydrase-ii inhibitors from marine macro brown alga *Dictyopteris hoytii* Supported by in silico studies *Molecules* 26:7074 doi:<https://doi.org/10.3390/molecules26237074>
32. Ramalingam S, Belani CP (2007) Role of bevacizumab for the treatment of non-small-cell lung. *cancer Future Med* 3:131–139. <https://doi.org/10.2217/14796694.3.2.131> .:2,
33. Rushdi MI, Abdel-Rahman IA, Saber H, Attia EZ, Abdelmohsen UR (2022) The natural products and pharmacological biodiversity of brown algae from the genus. Dictyopteris *J Mex Chem Soc* 66. <https://doi.org/10.29356/jmcs.v66i1.1639>
34. Schnitzler I, Boland W, Hay ME (1998) Organic sulfur compounds from *Dictyopteris* spp. deter feeding by an herbivorous amphipod (*Ampithoe longimana*) but not by an herbivorous sea urchin (*Arbacia punctulata*). *J Chem Ecol* 24:1715–1732. <https://doi.org/10.1023/A:1020876830580>
35. Selim SA (2012) Antimicrobial, antiplasmid and cytotoxicity potentials of marine algae *Halimeda opuntia* and *Sarconema filiforme* collected from Red Sea. *Coast World Acad Sci Eng Technol* 61:1154–1159
36. Song F, Fan X, Xu X, Zhao J, Yang Y, Shi J (2004) Cadinane sesquiterpenes from the brown alga *Dictyopteris divaricata*. *J Nat Prod* 67:1644–1649. <https://doi.org/10.1021/np040099d>
37. Song FH, Fan X, Xu XL, Zhao JL, Han LJ, Shi JG (2005) Chemical constituents of the brown alga Dictyopteris divaricata. *J Asian Nat Prod Res* 7:777–781. 10.1080/1028602032000169532
38. Toshi I, Koji Y, Tadashi M (1964) Sesquiterpenes from *Dictyopteris divaricata*. *I Bull Chem Soc Jpn* 37:1053–1055. 10.1246/bcsj.37.1053
39. Vega A, Rojano B, Blair S, Saez J (2008) Antimalarials and antioxidants compounds from *Piper tricuspe* (Piperaceae). *Pharmacologyonline* 1:1–8
40. Veikkola T, Karkkainen M, Claesson-Welsh L, Alitalo K (2000) Regulation of angiogenesis via vascular endothelial growth factor receptors. *Cancer Res* 60:203–212
41. Vinayak RC, Sabu A, Chatterji A (2011) Bio-prospecting of a few brown seaweeds for their cytotoxic and antioxidant activities. *J Evid-Based Integr Med* 2011. <https://doi.org/10.1093/ecam/neq024>

42. Wang H-S, Li H-J, Zhang Z-G, Wu Y-C (2018) Divergent synthesis of bioactive marine meroterpenoids by palladium-catalyzed tandem Carbene migratory insertion. *Eur J Org Chem* 2018:915–925. 10.1002/ejoc.201800026
43. Wright AD, Coll JC, Price IR (1990) Tropical marine algae, VII. The chemical composition of marine algae from North Queensland waters. *J Nat Prod* 53:845–861. <https://doi.org/10.1021/np50070a012>
44. Xu N, Fan X, Yan X, Tseng CK (2004) Screening marine algae from China for their antitumor activities. *J Appl Phycol* 16:451–456. 10.1007/s10811-004-5508-x
45. Zakaria Z et al (2019) Epidermal growth factor receptor (EGFR) gene alteration and protein overexpression in Malaysian triple-negative breast cancer (TNBC) cohort *OncoTargets. Ther* 12:7749–7756. 10.2147/OTT.S214611
46. Zhu H et al (2019) Synthesis of chalcone derivatives: inducing apoptosis of HepG2 Cells via regulating reactive oxygen species and mitochondrial pathway *Front pharmacol* 10. 10.3389/fphar.2019.01341

Figures

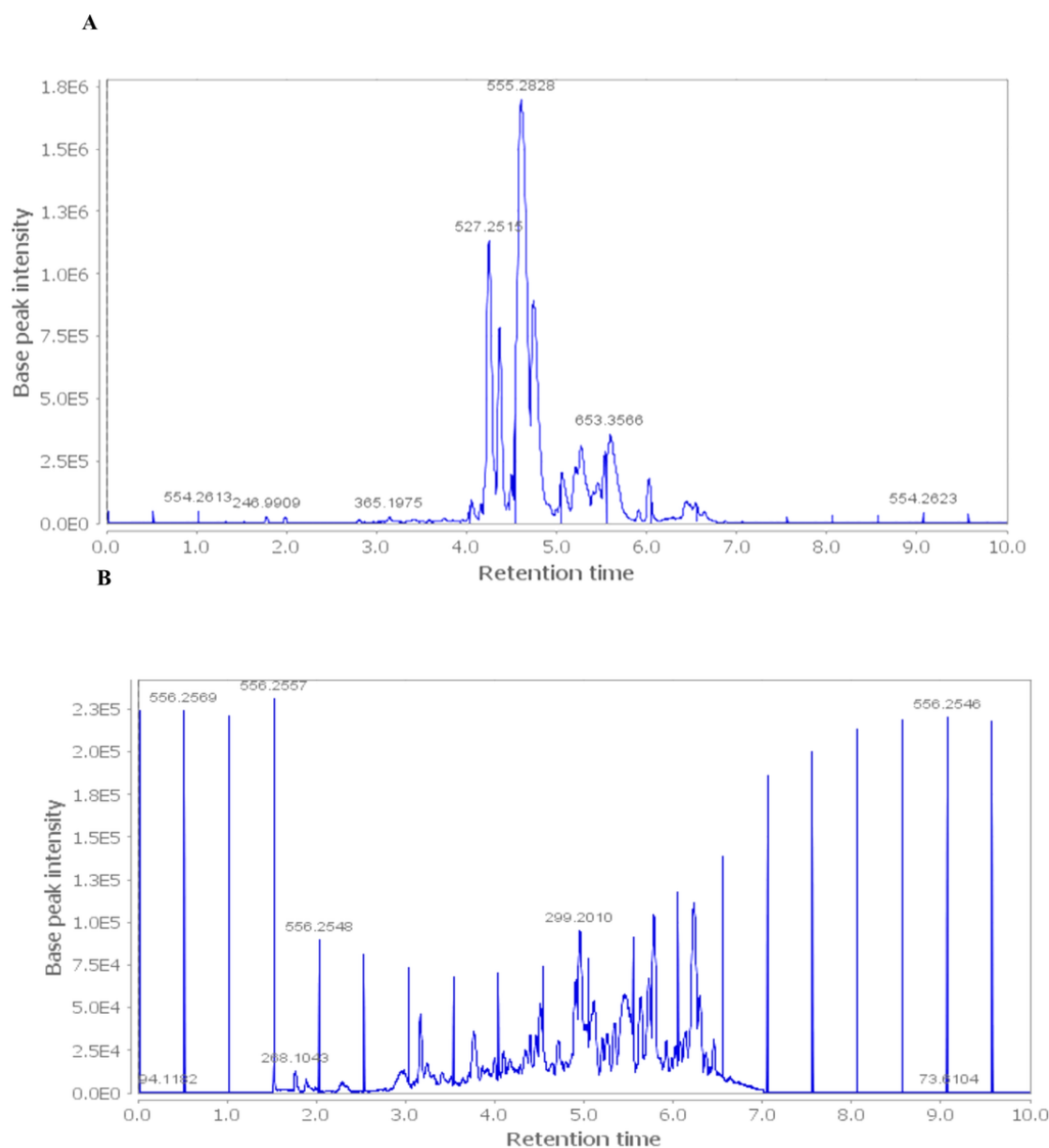


Figure 1

LC-HR-ESI-MS total ion chromatogram in negative mode (A) and positive mode (B) of the ethanol extract of *Dictyopteris acrostichoides*.

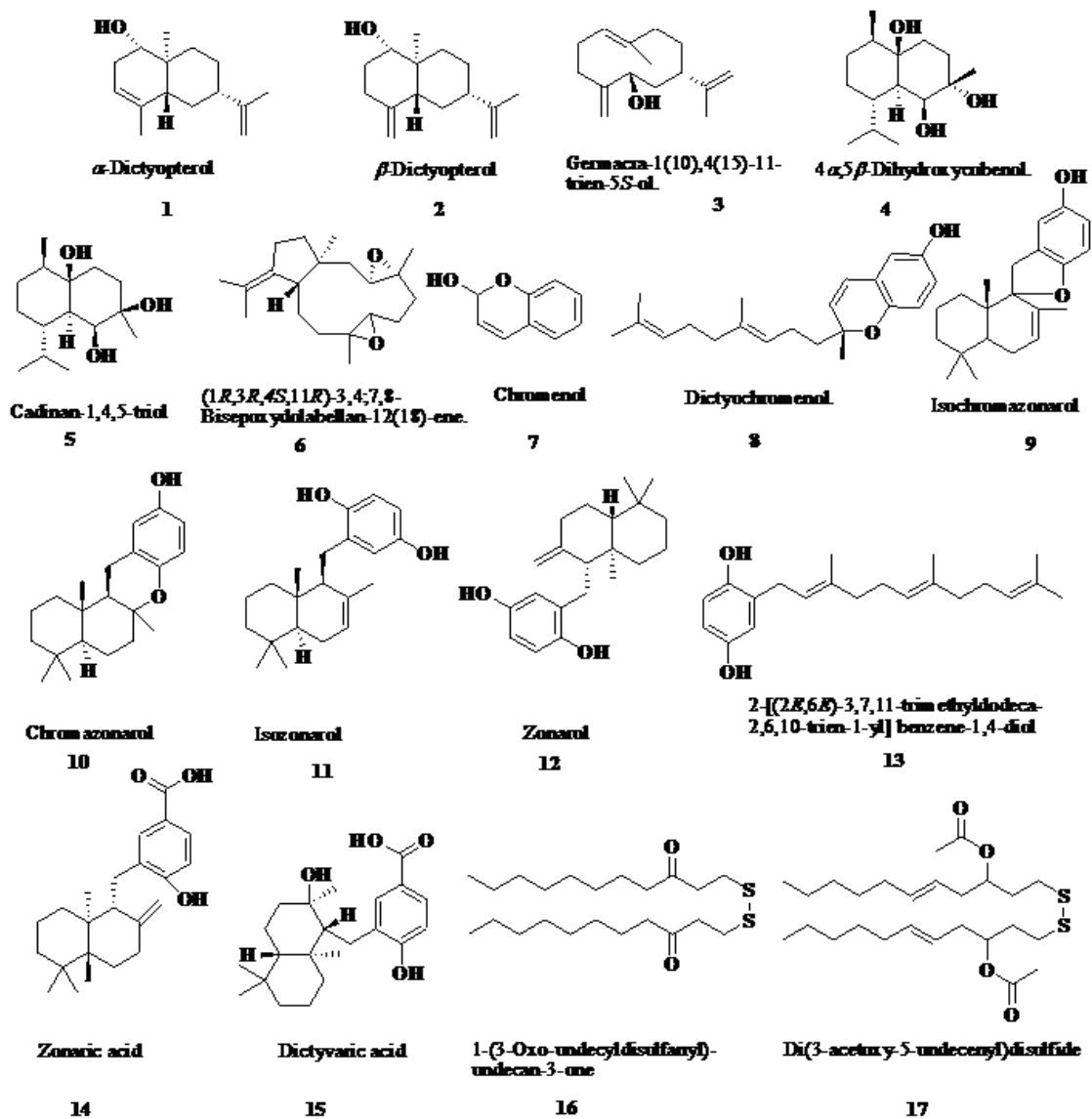


Figure 2

LC-HR-ESI-MS chemical structures of the ethanol extract of *Dictyopteris acrostichoides*.

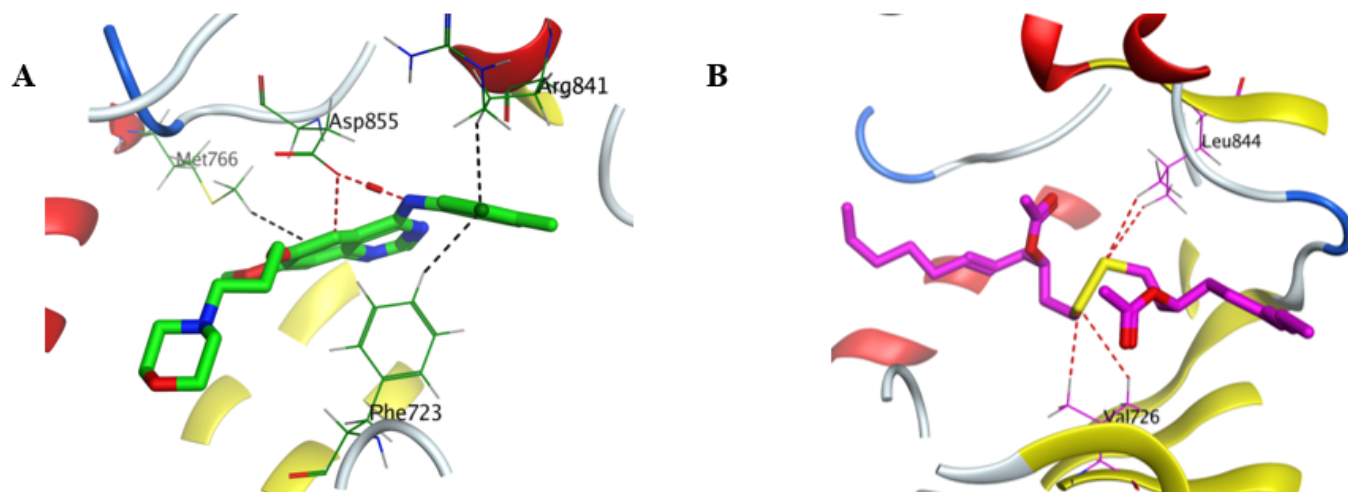


Figure 3

3D Docking poses of A and B into the gefitinib binding site in EGFR (PDB: 3UG2).

A: Compound (16) and B: Compound (17)

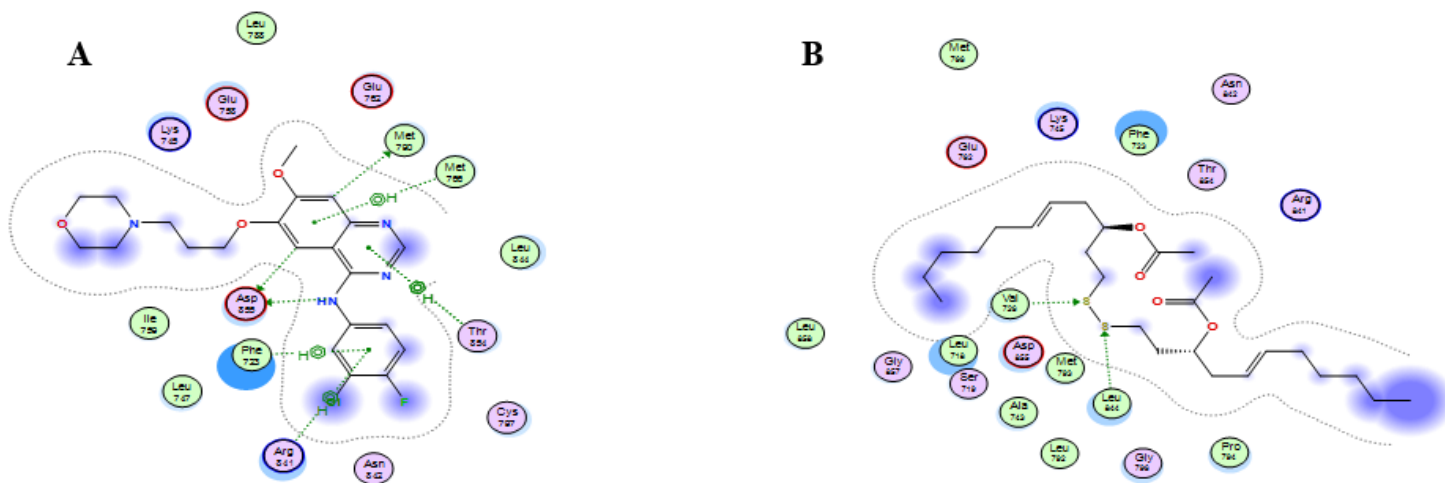


Figure 4

2D Docking poses of A and B into the gefitinib binding site in EGFR (PDB: 3UG2)

A: Compound (16) and B:Compound (17)

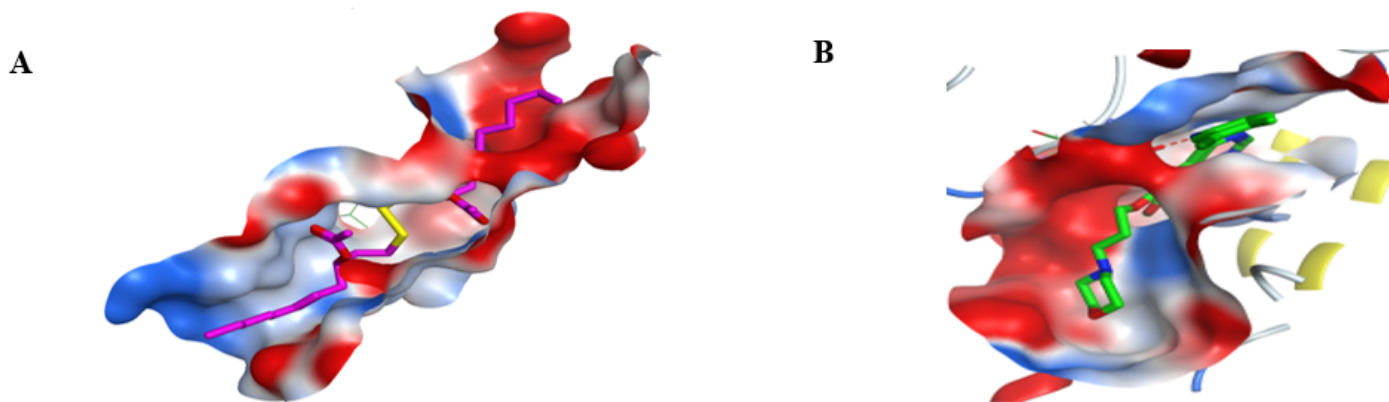


Figure 5

Surface and maps of the interaction potential of A and B into the gefitinib binding site in EGFR (PDB: 3UG2), A: Compound (17) and B: Gefitinib

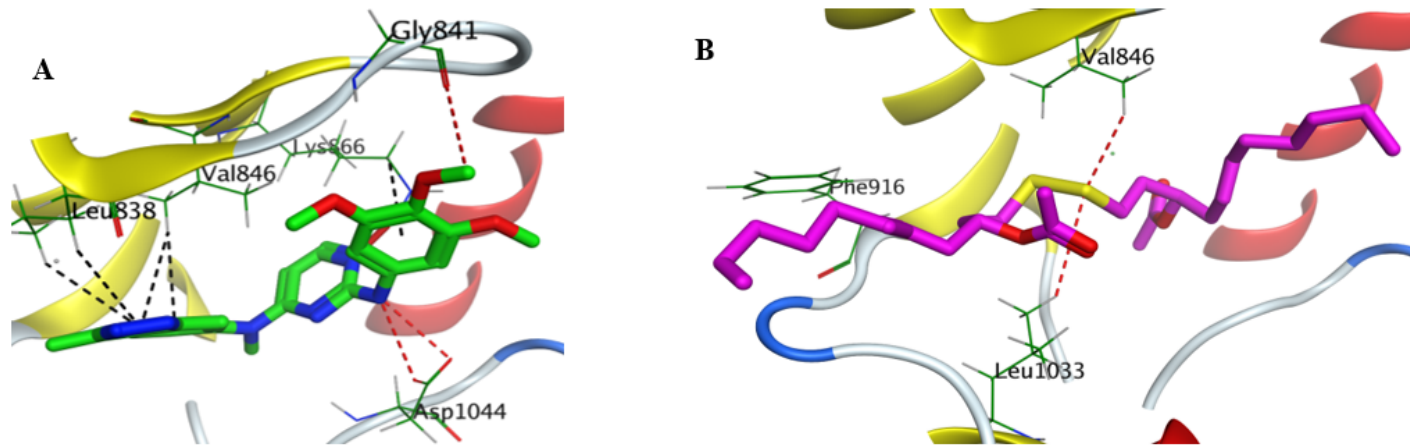


Figure 6

3D Docking poses of A and B into the KIM binding site in VEGFR (PDB: 3CJG).

A: Compound (17) and **B:** KIM

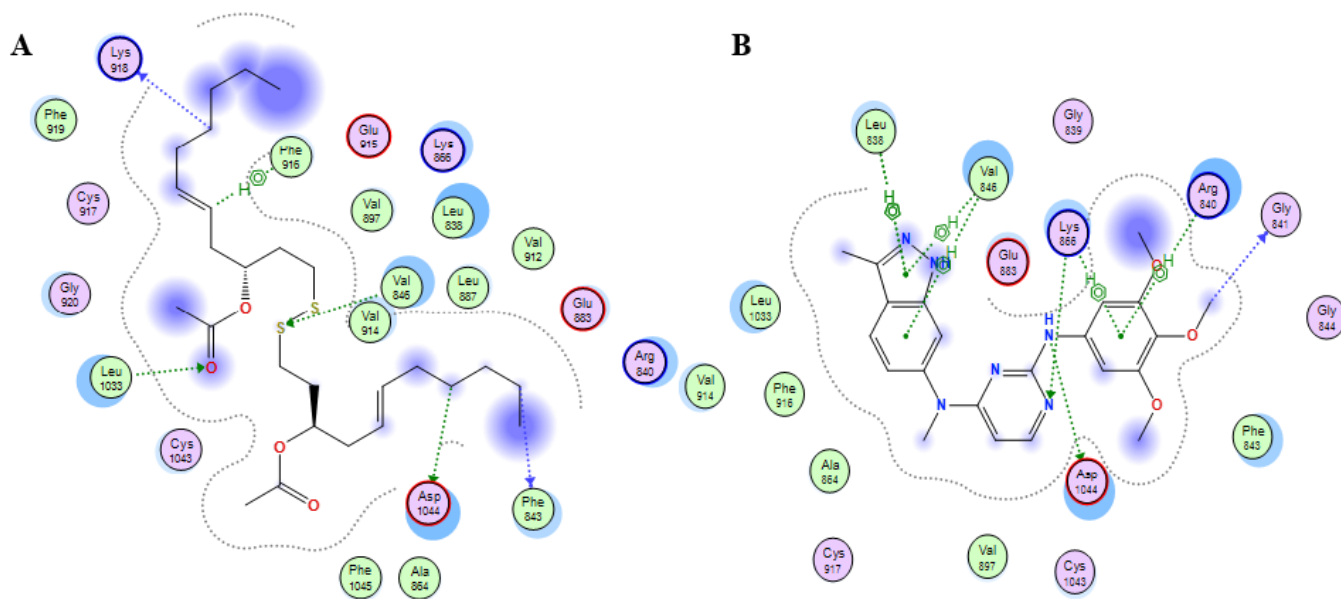


Figure 7

2D Docking poses of A and B into the KIM binding site in VEGFR (PDB: 3CJG).

A:Compound (17) and **B:** KIM

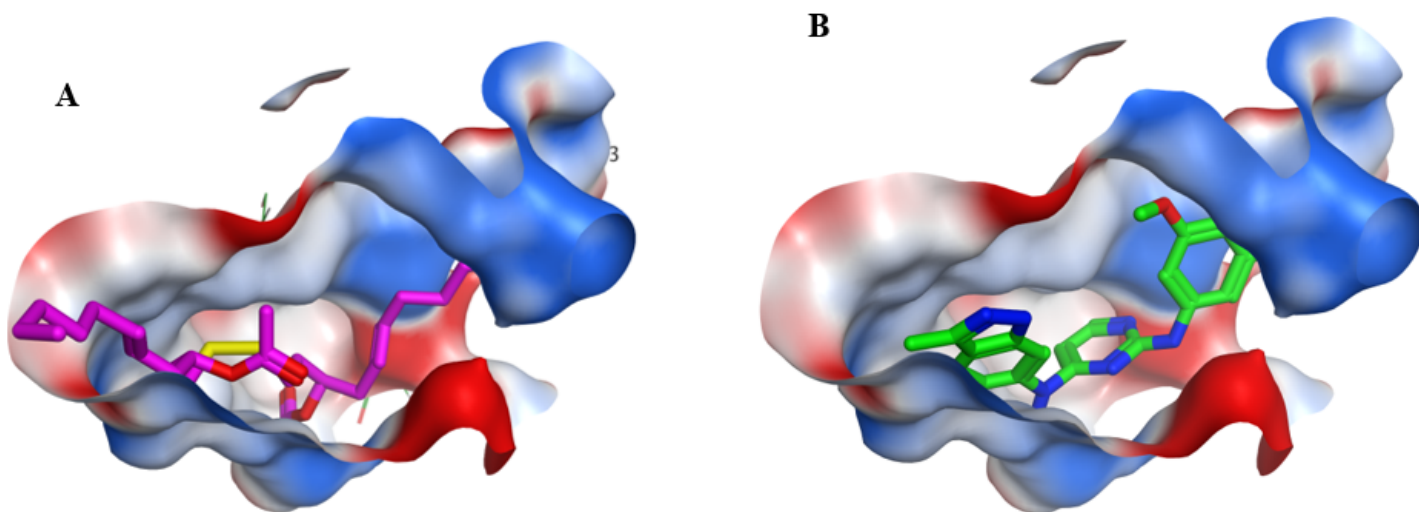


Figure 8

Surface and maps of the interaction potential of A and B into the KIM binding site in VEGFR (PDB: 3CJG).

A: Compound (17) and **B:** KIM

Supplementary Files

This is a list of supplementary files associated with this preprint. Click to download.

- [Graphabstract25042023.docx](#)